CP violating neutrino oscillation and uncertainties in Earth matter density

Lian-You Shan*

Institute of High Energy Physics, Chinese Academy of Sciences, P. O. Box 918, Beijing 100039, China
and CCAST (World Laboratory), P. O. Box 8730, Beijing 100080, China

Bing-Lin Young

Department of Physics and Astronomy, Iowa State University, Ames, Iowa 50011

Xinmin Zhang

Institute of High Energy Physics, Chinese Academy of Sciences, P. O. Box 918, Beijing 100039, China

We propose a statistical formulation to estimate possible errors in long baseline neutrino oscillation experiments caused by uncertainties in the Earth matter density. A quantitative investigation of the effect is made using the *CP* asymmetry in future experiments at the neutrino factory and superbeam.

I. INTRODUCTION

Leptonic *CP* violation (CPV) is one of the main challenges in future long baseline (LBL) neutrino oscillation experiments [1], where more precise measurements of the neutrino oscillation parameters are anticipated. However, since the neutrino beam travels a long path through Earth, the Mikheyev-Smirnov-Wolfenstein (MSW) matter effect [2], which is *CP* asymmetric and hence can mimic the *CP* effect, makes it nontrivial to extract the *CP* phase. Therefore a thorough delineation of the matter effect is necessary before an accurate account of the CPV effect can be achieved. However, the imprecise knowledge of Earth matter density which determines the electron number density (END) can be a major challenge in LBL experiments.

A number of approaches have been suggested for the treatment of Earth density profiles. We enumerate some of them: a distance-averaging effective constant [3], adiabatic approximation profile [4], mantle-core-mantle layers approximation [5], multistep functions [6], Fourier expansion around an average density [7], or the preliminary reference Earth model (PREM) [8]. We refer to Ref. [9] for a brief review of the available Earth density models from the viewpoint of the neutrino oscillation. It is not clear, however, if any of these approaches is sufficient for the accurate extraction of the *CP* phase.

It has been noted in some of the work that there is a length scale within which the density can be regarded as constant and the relevant physics is insensitive to mild local variations in the matter density. It should be commented that such a scale may depend on the values of the neutrino energy, the various mixing parameters, and the averaged matter density. All of these can contribute to uncertainties in the determination of the CP phase. Hence this length scale may vary case by case.

In this paper we consider another aspect of the matter density, i.e., its uncertainty at a given point on Earth from the

accepted model value. Such an uncertainty can affect the determination of the *CP* phase. As we will discuss in some detail below, this uncertainty is related to a length scale that defines the volume size within which a local model matter density is obtained by an averaging process. We will call this length scale the density uncertainty scale Δx. It is related to how the Earth matter density is determined in terms of geophysics measurements.

We propose, in this paper, an approach to estimate the error in the determination of the *CP* phase due to the uncertainty in the Earth matter density. The approach involves a weighted average over the sample space of possible Earth density profiles. Such a procedure is motivated by the consistent use of geophysical density data. A density model is an approximation of the Earth matter density and hence has its inherent uncertainties. For a brief discussion of the uncertainties in Earth density, and hence in the END, we refer to Refs. [5,10]. Specific cases of density uncertainties can be found in Ref. [11]. Detailed discussions of how to obtain the Earth matter density can be found in geophysics reviews [12–14]. Roughly speaking, the deeper it is toward Earth's center the closer the model density approaches the actual density. Meanwhile, the smaller the volume of Earth looked at, the less precisely can its local density be defined. The precision of the PREM is roughly 5% per $\Delta x \simeq 100$ km along the radial direction.

To model Earth matter uncertainty, we introduce a local variance function $\sigma(x)$ to characterize the uncertainty at each point on Earth along a given baseline. Given the variance function we can sample Earth density profiles and construct an averaging process to calculate the resultant deviation of a physical quantity from its mean value. The probability of the various END samples is taken as a logarithmic distribution which is suitable for non-negative quantities, although other statistical approaches may be used. We will also show that the conventional approach using a fixed deviation of Earth matter density tends to overestimate the *CP* uncertainties and renders the determination of the *CP* phase very difficult. This offers an explicit example to show that how we treat the uncertainties of the Earth matter den-

---

*Email address: shanly@ihep.ac.cn

66 053012-1

sity can affect the analysis of the neutrino CP phase and possibly other mixing parameters too.

In Sec. II we present our formulation of the error estimate. Section III presents the numerical results. A brief summary is given in Sec. IV.

II. FORMULATION FOR ERROR ESTIMATE

We begin with the formulation of the flavor Hamiltonian that governs the propagation of the neutrino in matter. The time, or equivalently the distance, evolution of the neutrino along its path is given by the Schrödinger equation

$$i\frac{\partial \nu_f}{\partial x} = H\nu_f, \tag{1}$$

where x is the distance traveled by the neutrino, and ν_f is a column matrix containing n flavor eigenstates of neutrinos. Omitting terms leading only in a common phase in all flavor states and in the scheme of three flavors of neutrinos in the order of ν_e, ν_μ, and ν_τ, we have the distance dependent Hamiltonian

$$H[\delta_{CP}, N_e(x)] = \frac{U}{2E_\nu} \begin{pmatrix} m_1^2 & 0 & 0 \\ 0 & m_2^2 & 0 \\ 0 & 0 & m_3^2 \end{pmatrix} U^\dagger$$

$$+ \begin{pmatrix} \sqrt{2}G_F N_e(x) & 0 & 0 \\ 0 & 0 & 0 \\ 0 & 0 & 0 \end{pmatrix}, \tag{2}$$

where E_ν is the energy of the neutrino, G_F the Fermi constant, and m_j, $j=1$, 2, 3, the neutrino mass eigenvalues. We have exhibited the functional dependences of H that we focuson in the present discussion, i.e., δ_{CP} and $N_e(x)$. δ_{CP} is the CP phase angle. $N_e(x)$ is the electron number density function, usually referred to as the END function, which depends on the Earth matter density and determines the matter effect in neutrino oscillations. U is the three-neutrino mixing matrix which relates neutrino mass eigenstates to their flavor eigenstates, in the basis where the charged leptons are diagonalized. A parametrization of U [15,16] is

$$U = \begin{pmatrix} c_{12}c_{13} & c_{13}s_{12} & \hat{s}_{13}^* \\ -c_{23}s_{12} - c_{12}\hat{s}_{13}s_{23} & c_{12}c_{23} - s_{12}\hat{s}_{13}s_{23} & c_{13}s_{23} \\ s_{12}s_{23} - c_{12}c_{23}\hat{s}_{13} & -c_{12}s_{23} - c_{23}s_{12}\hat{s}_{13} & c_{13}c_{23} \end{pmatrix} \tag{3}$$

where $s_{jk} = \sin(\theta_{jk})$, $c_{jk} = \cos(\theta_{jk})$, $\hat{s}_{jk} = \sin(\theta_{jk})e^{i\delta_{cp}}$, $j,k=1$, 2, and 3, and θ_{jk} are the mixing angles. For the antineutrino, $N_e(x)$ is replaced by $-N_e(x)$ and U by its complex conjugate. The latter is equivalent to replacing δ_{CP} by $-\delta_{CP}$.

In a medium of varying density profile, like H in Eq. (2), one has to find an appropriate approximate treatment, or numerically integrate Eq. (1), to obtain the oscillation probability amplitude. However, the formal solution of a time depen-

dent Hamiltonian is well known. The oscillation probabilities can be written as, for a given END,

$$\mathbf{P}_{\alpha\beta}[\mathbf{N}_e] \equiv P_{\nu_\alpha \to \nu_\beta}(L, E_\nu, \delta_{CP}, \mathbf{N}_e)$$

$$= \left| \left(\mathcal{T}\exp\left(-i\int_0^L H[\delta_{CP}, N_e(x)]dx \right) \right)_{\alpha\beta} \right|^2,$$

$$\mathbf{P}_{\bar{\alpha}\bar{\beta}}[\mathbf{N}_e] \equiv P_{\bar{\nu}_\alpha \to \bar{\nu}_\beta}(L, E_\nu, \delta_{CP}, \mathbf{N}_e)$$

$$= \left| \left(\mathcal{T}\exp\left(-i\int_0^L H[-\delta_{CP}, -N_e(x)]dx \right) \right)_{\alpha\beta} \right|^2, \tag{4}$$

where L is the baseline and $\mathcal{T}$ denotes the path-ordered product [17]. $N_e(x)$ is the END as a function of x. On the left-hand sides, $\mathbf{N}_e$ denotes explicitly the functional dependence of oscillation probabilities on the END, and hence the fact that any uncertainties in Earth matter density can lead to errors in the measurement of oscillation parameters, including the leptonic CPV phase.

Although the END is a critical factor in the analysis of the long baseline oscillation data, what is available is an averaged Earth density function $\hat{N}_e(x)$ with some prescribed errors, such as the widely used PREM model.[1] However, what the neutrino experiences as it propagates in Earth is likely to be a medium with a density that deviates in some degree from the average value. A straightforward, conventional way to deal with the density deviation is to assign a distance independent error to $\hat{N}(x)$. Because of the oscillating nature of the probability function, it is not clear that a constant deviation is appropriate. In the following we propose an approach to study the effect of density uncertainties. Our approach tries to mimic how the END is obtained from geophysical data.

Let us define the average density $\hat{N}_e(x)$ as an average over all samples of the density profiles $\{N_e(x)\}$, and its uncertainty $\sigma(x)$ as usual as a variance function. Using the notation of the functional integral, we have

$$\hat{N}_e(x) \equiv \langle N_e(x) \rangle = \int [\mathcal{D}N_e(x)]N_e(x)F[N_e(x)], \tag{5}$$

$$\sigma(x) \equiv \sqrt{\langle N_e^2(x) \rangle - \langle N_e(x) \rangle^2}, \tag{6}$$

where $[\mathcal{D}N_e(x)]F[N_e(x)]$ is the probability of obtaining the END profile $N_e(x)$ in the neighborhood Δx around x. The actual oscillation probability is the average over all possible END profiles $N_e(x)$. The appropriate framework for such a statistical expectation is the functional integration formulation in which Earth density profiles span a functional space that contains all possible variations of Earth densities al-

---

[1]There are more updated Earth density models available such as the AK135 [18] model, which has notable differences from the PREM model. We use the PREM for the purpose of illustration.

lowed by the given variance and weighted by a distribution function $F[N_e(x)]$. We can write

$$\langle \mathbf{P}_{\alpha\beta} \rangle \equiv \int [\mathcal{D}N(x)_e] F[N_e(x)] \mathbf{P}_{\alpha\beta}[\mathbf{N}_e]. \qquad (7)$$

We will describe how to evaluate this expression later near the end of this section.

To determine the average Earth matter density as is done in geophysics, a uniform random sampling in the space of possible matter density profiles is used to generate a matter density model [19,20]. The density function so generated is tested against two important sets of observational data. One set of observational data is Earth's total mass together with its moment of inertia, and the other is the normal modes of Earth's free oscillation. In general the samples so obtained approach a Gaussian, i.e., normal, distribution, rather than a uniform one. This, together with the fact that Earth matter density is always positive, suggests that we use a logarithmic normal distribution to represent the Earth's matter density probability [21]:

$$F[N_e(x)] = \frac{1}{N_e(x)\sqrt{2\pi}s(x)} \exp\left(-\frac{\ln^2[N_e(x)/N_0(x)]}{2s^2(x)}\right), \qquad (8)$$

$$s(x) = \sqrt{\ln[1+r^2(x)]}, \quad N_0(x) = \hat{N}_e(x)\exp[-s^2(x)/2], \qquad (9)$$

where

$$r(x) = \sigma(x)/\hat{N}_e(x) \qquad (10)$$

parametrizes the uncertainty in the END in terms of the ratio of the local variance and the local mean value of the Earth density. What we mean by *local* is the neighborhood Δx which contains a finite but sizable volume. We will refer to the uncertainty defined by Eqs. (10) and (9) as the *weighted matter uncertainty*, although $r(x)$ can be a fixed value.

At a given point x along the path of the neutrino, we use Monte Carlo calculations to generate the value of the weighting functional $F[N_e(x)]$ which is a number lying between 0 and 1. With the chosen averaged density function $\hat{N}_e(x)$ and the error variance $r(x)$, the values of the functions $s(x)$ and $N_0(x)$ can be computed by Eqs. (9) and (10). Hence the value of the density function $N_e(x)$ can be obtained from Eq. (8). The formulation can then be applied to investigate the effect of the matter density uncertainties on data fitting of oscillation variables.

The logarithmic distribution is not a symmetric distribution for arbitrary σ. However, it is close to the Gaussian distribution when σ is much smaller than $\hat{N}_e(x)$, i.e., small $r(x)$. In Fig. 1 we plot the logarithmic and Gaussian distributions for constant $r(x)$ of 0.05 and 0.50 with $\hat{N}_e(x)$ given by the PREM. The difference between the Gaussian and the logarithmic distributions is very small in the case of small $r(x)$ such as $r(x)=0.05$. However, for large $r(x)$, e.g., $r(x)=0.50$, the difference between the two distributions is large. Since we take only small error invariances $r(x)$, the

present formulation always deals with normal-like distributions. For simplicity, we will use a constant weighted matter uncertainty throughout the present work. Furthermore, since 5% is the precision of the PREM, we will take $r(x) = 0.05$.

In Fig. 2, we plot the density profiles for weighted uncertainty $r(x)=0.05$. The thick solid line is the PREM value [22] which is the weighted average, Eq. (5), of the density samples, $N_e(x)$, that are generated by Eq. (8) and shown by the rapidly oscillating thin lines. To compare with the generally used fixed matter density uncertainty of range $2r'(x)$,

$$N_e'(x) = [1 \pm r'(x)]\hat{N}_e(x), \qquad (11)$$

we also plot $[1+r'(x)]\hat{N}_e(x)$ in Fig. 2 with a constant [23,24] $r'(x)=5\%$ by the dotted line, where $[1-r'(x)]\hat{N}_e(x)$ will lie below the PREM curve almost symmetrically with $[1+r'(x)]\hat{N}_e(x)$. We will refer to $r'(x)$ as the *fixed matter uncertainty* to distinguish it from $r(x)$. $r(x)$ is associated with $N_e(x)$ and $r'(x)$ with $N_e'(x)$.

Given the matter density uncertainties and PREM, we can compute the uncertainty to the neutrino oscillation probability by its variance,

$$\delta P_{\alpha\beta} \equiv \sqrt{\langle (P_{\alpha\beta} - \langle P_{\alpha\beta} \rangle)^2 \rangle}$$

$$= \sqrt{\int [\mathcal{D}N_e] F[N_e(x)] (P_{\alpha\beta} - \langle P_{\alpha\beta} \rangle)^2}. \qquad (12)$$

The variance $\delta P_{\alpha\beta}$ allows us to estimate the uncertainty of a physical quantity, such as the leptonic *CP* phase, caused by the uncertainty in matter density. Usually, one measures the difference between the event rates of the neutrino and antineutrino of a given flavor to search for the CPV effect,

$$N_{CP}(L, E_\nu, \delta_{CP}, N_e(x)) \equiv N_\beta - N_{\bar{\beta}}$$

$$= \mathcal{N}_0 [\phi_{\nu_\alpha}(L, E_\nu) P_{\alpha\beta} \sigma_\beta(E) T_D$$

$$- \phi_{\bar{\nu}_\alpha}(L, E_\nu) P_{\bar{\alpha}\bar{\beta}} \sigma_{\bar{\beta}}(E_\nu) \bar{T}_D] \Delta E$$

$$= \mathcal{N}_0 \phi_{\nu_\alpha}(L, E_\nu) D_{\alpha\beta}^{CP}(\delta_{CP}, N_e(x))$$

$$\times \sigma_\beta(E_\nu) T_D \Delta E_\nu, \qquad (13)$$

where $\mathcal{N}_0$ is a normalization factor with unit conversions, $\phi_{\nu_\alpha}(L, E_\nu)$ [$\phi_{\bar{\nu}_\alpha}(L, E_\nu)$] is the neutrino (antineutrino) beam flux spectrum of flavor α ($\bar{\alpha}$), $\sigma_\beta(E_\nu)$ [$\sigma_{\bar{\beta}}(E_\nu)$] is the charged current cross section of neutrino (antineutrino) of flavor β ($\bar{\beta}$), T_D ($\bar{T}_D$) is the product of the running time and detector size of the neutrino (antineutrino) beam, and ΔE_ν is the energy bin size. We have assumed that the neutrino and antineutrino beams have the same flux spectrum and the mass of the detector for the antineutrino is twice that of the neutrino so as to compensate the difference in the neutrino and antineutrino charged current cross sections. We have also adopted a *CP*-odd difference [25,3,4] defined by
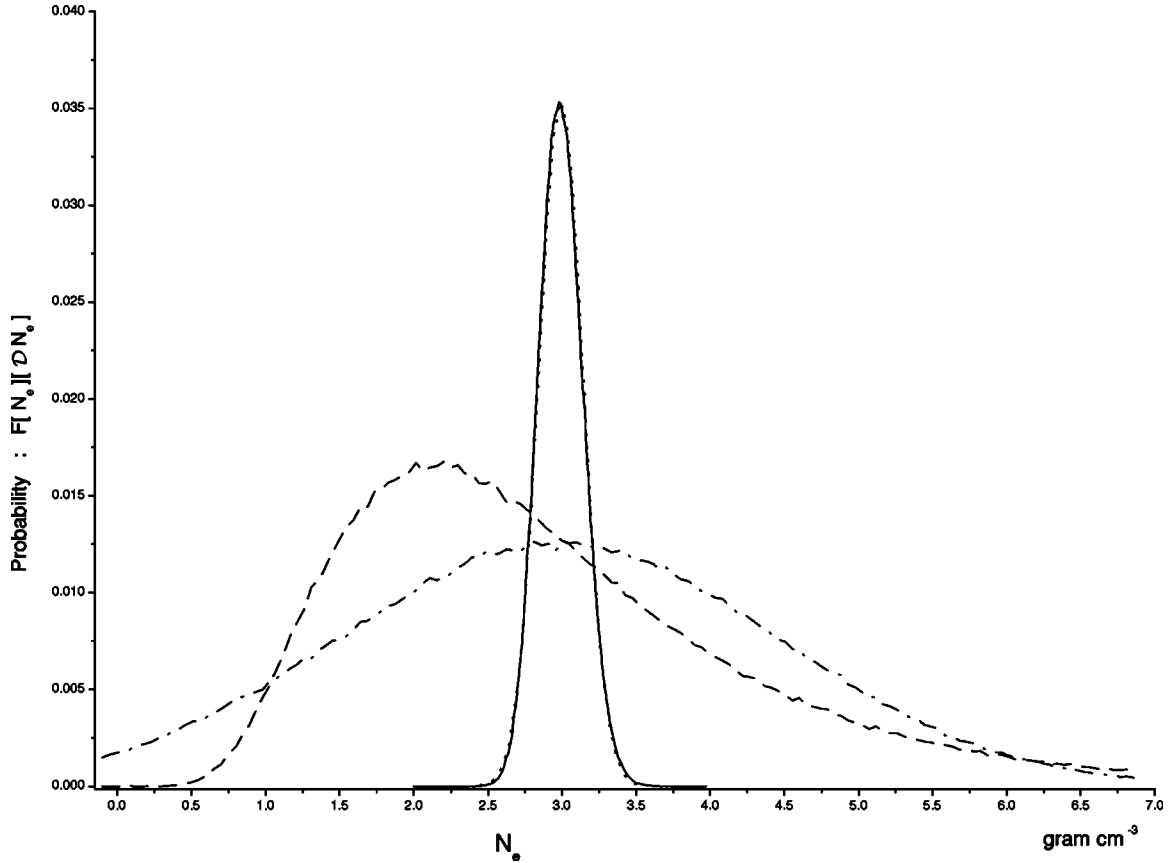
FIG. 1. Plot of probability distribution $F[N_e(x)][\mathcal{D}N_e(x)]$ vs density $N_e(x)$ at depth, e.g., $R = 6200$ km from the Earth surface. The mean value is taken from the PREM which is 3 g/cm^3. The solid and dotted lines are the logarithmic and Gaussian distributions with $r = 5\%$, which almost coincide. The dash and dash-dotted lines are the logarithmic and Gaussian distribution for $r = 50\%$, respectively, which show that the two distributions differ significantly and the Gaussian distribution involves negative density.

$$D_{\alpha\beta}^{CP}[\delta_{CP}, N_e(x)] \equiv P_{\nu_\alpha \to \nu_\beta}(L, E_\nu, \delta_{CP}, N_e(x))$$
$$- P_{\bar{\nu}_\alpha \to \bar{\nu}_\beta}(L, E_\nu, \delta_{CP}, N_e(x)), \tag{14}$$

where the notation for the E_ν and L dependence has been suppressed on the left-hand side.

The uncertainty in the matter density gives rise to an uncertainty in the event number difference,

$$\delta N_{CP}(L, E_\nu, \delta_{CP}, N_e(x))$$
$$\equiv \mathcal{N}_0 \phi_{\nu_\alpha}(L, E_\nu) \delta D_{\alpha\beta}^{CP}[\delta_{CP}, N_e(x)] \sigma_\beta(E_\nu) T_D \Delta E_\nu, \tag{15}$$

where

$$\delta D_{\alpha\beta}^{CP}[\delta_{CP}, N_e(x)] \equiv \sqrt{\langle [(P_{\alpha\beta} - P_{\bar{\alpha}\bar{\beta}}) - \langle (P_{\alpha\beta} - P_{\bar{\alpha}\bar{\beta}}) \rangle]^2 \rangle}$$
$$= \sqrt{[\delta P_{\alpha\beta}]^2 + [\delta P_{\bar{\alpha}\bar{\beta}}]^2}. \tag{16}$$

We need a criterion to tell us when the variance is under control so that a CP phase can possibly be extracted. To do that we require in a given energy bin

$$\left| \frac{\delta D_{\alpha\beta}^{CP}}{\Delta D_{\alpha\beta}^{CP}} \right| < 1, \tag{17}$$

where

$$\Delta D_{\alpha\beta}^{CP} \equiv D_{\alpha\beta}^{CP}[\delta_{CP}, \hat{N}_e(x)] - D_{\alpha\beta}^{CP}[\delta_{CP} = 0, \hat{N}_e(x)] \tag{18}$$

which crudely measures the "pure" CP effect. Unless Eq. (17) is satisfied, it will be difficult to distinguish the effect of a finite CPV phase from that of vanishing δ_{CP} due to the error caused by the uncertainty of the matter density. The conventional estimate based on Eq. (11) gives an error variance of the form

$$\delta D_{\alpha\beta}'^{CP} \equiv D_{\alpha\beta}^{CP}[\delta_{CP}, N_e'(x)] - D_{\alpha\beta}^{CP}[\delta_{CP}, \hat{N}_e(x)]. \tag{19}$$

Our estimate in Eq. (16) contains an average and can better mimic the realistic Earth density model. We will see in the next section that our estimate leads to a more controllable error variance of the CP phase than that of the conventional estimate, Eq. (19).

We evaluate Eqs. (7) and (16) numerically using a method similar to that of lattice gauge theory. This is a one-dimensional problem with a few parameters, so it is much
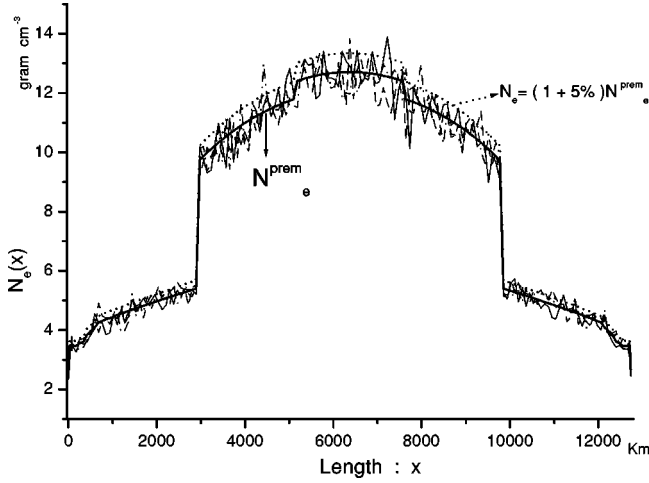
FIG. 2. Plots of Earth matter density along a diameter from one end on the Earth surface to the opposite end. The thick solid line is for $\hat{N}_{e(x)}$ [22] which we take to be the PREM. The dotted line above $\hat{N}_{e(x)}$ is $N_e(x) = (1 + 5\%)\hat{N}_e(x)$. The rapidly oscillating lines are sample profiles generated according to Eq. (9) with $r(x) = 5\%$.
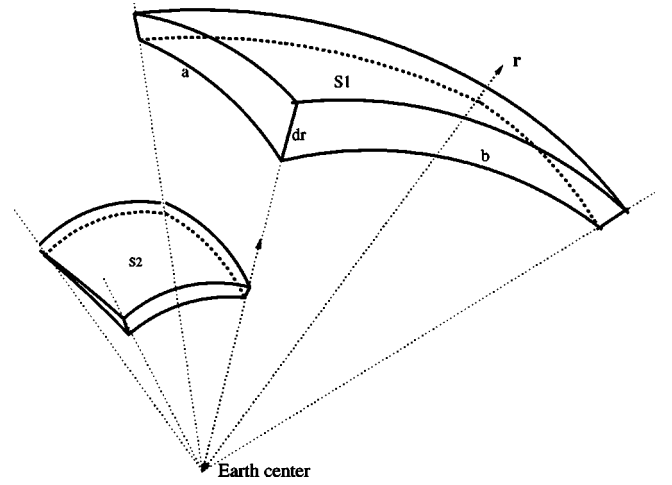

FIG. 3. A schematic diagram for the scale to define density and its uncertainty. a or b is larger than dr, while $S2$ is smaller than $S1$ with decreasing radius.

simpler. The neutrino path is discretized into I cells, where I is determined by the relevant geophysics information. In each of the cells, the averaged END function $\hat{N}_e(x_i)$ and the local variance $\sigma(x_i)$ are known, where x_i is the center point of the ith cell. $F[N_e(x_i)]$ is generated by Monte Carlo simulation. Then $N_e(x_i)$ can be solved from Eq. (9), and a density function $N_e(x)$ can be approximated by a series of density steps $N_e(x_1), \ldots, N_e(x_i), \ldots, N_e(x_I)$. For not too large local variance $\sigma(x_i)$ the distribution will be normal, Gaussian like.

The estimators of the mean and the deviation can be recast respectively into the forms

$$\langle D_{\alpha\beta}^{CP} \rangle = \lim_{I \to \infty} \int \prod_{i=1}^{I} [\mathcal{D}N_e(x_i)] F[N_e(x_i), x_i] D_{\alpha\beta}^{CP}[\delta_{CP}; \mathbf{N}_e]$$

$$= \lim_{K \to \infty} K^{-1} \sum_{k=1}^{K} \tilde{D}_k[\delta_{CP}; \{N_e\}_k], \tag{20}$$

$$\delta D_{\alpha\beta}^{CP} = \left(\lim_{K \to \infty} (K-1)^{-1} \sum_{k=1}^{K} (\tilde{D}_k - \langle D_{\alpha\beta}^{CP} \rangle)^2 \right)^{1/2}. \tag{21}$$

In the third line of Eq. (20), as usual, we have replaced the functional integration by averaging over K density profiles. We denote the array $\{N_e\}_k$ $\equiv \{N_e(x_1), \ldots, N_e(x_i), \ldots, N_e(x_I)\}_k$ for $k = 1, \ldots, K$, where each array $\{N_e\}_k$ is generated according to the distribution $F[N_e]$ by the method of importance sampling as described above. $\tilde{D}_k$ is evaluated on such density arrays. We

have checked numerically that Eqs. (20) and (21) are convergent and stable against further increase in K when K is large enough.

Three comments are in order. First, the use of the arrays $\{N_e\}_k$ also allows the formulation to accommodate the real-time density variations over the neutrino trajectories due to other factors, such as temperature variations. However, such variations are usually small. Second, in geophysics, to obtain the density profile, Earth is discretized into hexahedrons, which are elementary volumes in spheroidal coordinates, as shown in Fig. 3. The Earth density is calculated on the nodes[2] of the hexahedron as an inverting problem [28,12,21]. Limited by the accuracy of geophysics data and computational facilities, a cutoff in the size of the hexahedrons Δx is imposed. For a very long neutrino trajectory that goes nearly along the Earth diameter, the length scale is about 100 km. For a neutrino trajectory very near to the Earth surface, the length scale can be large since the neutrino travels mainly in the lateral direction, staying mostly within a given hexahedron where the homogeneity is small. In both cases I is determined. Third, since the series in Eqs. (20) and (21) converges rapidly for not too large $r(x)$ due to the Gaussian-like distribution of Eq. (9), for a guide to the computation one can identify K roughly with the number of beam neutrinos in the individual bins, i.e.,

$$K \equiv K(L, E_\nu) = \phi_{\nu_\alpha}(L, E_\nu) \sigma_\alpha(E_\nu) \Delta E_\nu. \tag{22}$$

However, we found that in general K of the order of several thousand, say, 5000, is sufficient.

Let us also mention that we have checked our numerical approach by examining the MSW resonance in two neutrino flavors. By choosing a mixing angle and matter density we can determine analytically the resonance energy and the shortest baseline at the resonance energy so that the probabil-

---

[2]A node is a point where three lines intersect; hence it is a corner of the hexahedron. There are eight nodes for a hexahedron.

ity is unit. We use this resonance baseline and calculate the probability and event number as a function of the neutrino energy according to Eq. (7) with $r(x) = 5\%$. We reproduce the analytic result to a good degree of precision, including the unity probability at the resonance energy and other maxima of the probability of value less than 1 below the resonance energy.

In the above discussion we have ignored other contributions to the error. In the presence of other errors, we have to do a better job in estimating the contribution of the matter density uncertainty to the error and make a χ^2 analysis which we briefly explore below. We define a fractional error variance

$$\sigma_{\text{den}}(E,L) \equiv \frac{\delta N_{CP}[\delta_{CP}, N_e(x)]}{\mathcal{E}_{\text{tot}}} \quad (23)$$

where $\mathcal{E}_{\text{tot}}$ is the total systematic error. To measure this systematic error, we adopt the following qualitative χ^2 analysis. Define

$$S_{jl} = s_j s_l + \rho_{jl} \sigma_{\text{den},j} \sigma_{\text{den},l}, \quad (24)$$

$$\chi^2 = \sum_{j,l=1}^{J} \{N_j^{\text{expt}} - N_j^{\text{theo}}[\delta_{CP}, \hat{N}_e(x)]\}$$

$$\times (S^{-1})_{jl}\{N_l^{\text{expt}} - N_l^{\text{theo}}[\delta_{CP}, \hat{N}_e(x)]\}, \quad (25)$$

where j and l label the energy bins when the data is analyzed over a range of energies.[3] s_j is the statistical error in the jth bin. The term $\rho_{jl} \sigma_{\text{den},j} \sigma_{\text{den},l}$ denotes possible correlations between the jth and lth bins. As in [26], N_j^{expt} as defined in Eq. (13) is the observed event number in the jth bin, and $N_j^{\text{theo}}[\delta_{CP}, \hat{N}_e(x)]$ is the corresponding event number estimated theoretically for the CP angle δ_{CP} and the density profile $\hat{N}_e(x)$. One might think that the matter density uncertainty merely contributes to the error of δ_{CP} but does not change the best-fit value of δ_{CP}. However, this is not the case if $\sigma_{\text{den},j}$ is not an overall constant independent of j. When $\sigma_{\text{den},j}$ varies from bin to bin, the correlation coefficient ρ_{jl} will be nonvanishing although smaller than unity, the χ^2 will change, and hence the best-fitted value of δ_{CP} will also be changed [27,26]. The χ^2 cannot be quantitatively determined until one can access experimental leptonic CPV data. So we will not dwell on it further in the present work.

III. NUMERICAL RESULTS

In the following numerical calculation we take the baseline to be 2900 km. This baseline was suggested as an appropriate distance for the study of the CP effect at a neutrino factory [29]. We also present some of the results for a very long baseline of 12000 km for comparison. Needless to say, our formulation also applies to the superbeam [30]. For the

_____

[3] We note that the j and l sums can represent sums over other variables, such as baselines if the data of several baselines are analyzed jointly.
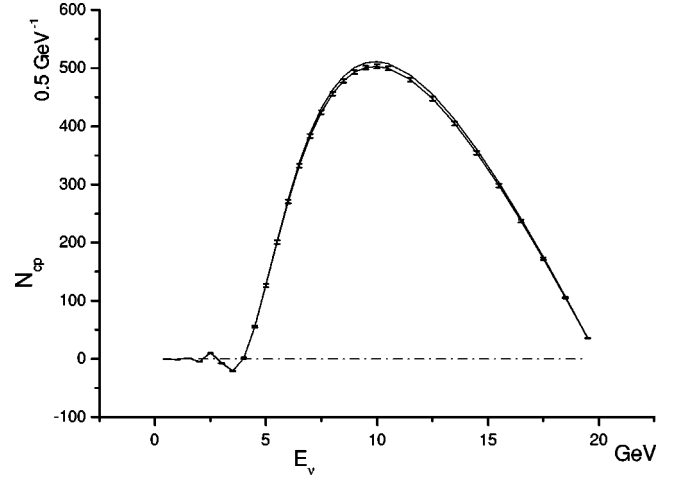

FIG. 4. Plot of CP-odd event number difference N_{CP} vs neutrino energy E_ν for baseline $L = 2900$ km. The dashed line with error bars is for $\delta_{CP} = 0°$ and the error bars represent the variance caused by the uncertainty of matter density with $r = 5\%$. The solid line without error bars is the prediction of $\delta_{CP} = 7.5°$ in the PREM, i.e., $r(x) = 0$.

neutrino beam we assume a 20 GeV high performance neutrino factory, which delivers 10^{21} working muons per year. For the detector and running time we use a conservative $T_D = 1 \times 50$ kton yr. We adopt the large mixing angle scenario [31] for the solar neutrino and take the following typical set of mixing parameters:

$$\Delta m_{\text{sol}}^2 = 6.0 \times 10^{-5} \text{ eV}^2, \quad \Delta m_{\text{atm}}^2 = 3.55 \times 10^{-3} \text{ eV}^2,$$

$$\sin^2 2\theta_{13} = 0.08, \quad \tan^2 \theta_{12} = 0.3, \quad \sin^2 2\theta_{23} = 0.99. \quad (26)$$

For the investigation of the CP effect at the neutrino factory, it is most advantageous to observe the so-called wrong sign muons, i.e., the muon signals from $\nu_e \rightarrow \nu_\mu$ in an antimuon storage ring together with the antimuon signals from $\bar{\nu}_e \rightarrow \bar{\nu}_\mu$ in a muon storage ring. For the 2900 km baseline, the deepest point of the neutrino path in the Earth along the radial direction is 167 km. This reaches only the low velocity region of the mantle. Such a path is still rather near to the surface of the Earth surface, but the uncertainty of the PREM can be significant, of the order of $r(x) = 5\%$. We take the distance uncertainty scale $\Delta x \simeq 200$ km.

Now we present the numerical results. First, we study the extent to which the matter effect can mimic the CPV effect and the effect of the weighted variance distribution approach proposed in this article. In Fig. 4, we plot the event number difference N_{cp} defined in Eq. (13) as a function of the neutrino energy, comparing the results of vanishing and finite δ_{CP}, in vacuum and in Earth medium. The dash-dotted flat line for $N_{CP} = 0$ is for the vacuum for $\delta_{CP} = 0$. The solid curve attached with error bars is for Earth medium also with vanishing CP phase angle. The difference between this curve and the vacuum current clearly shows the MSW matter effect. The error bars are given by $r = 5\%$ in the PREM, estimated in the weighted variance distribution given in Eqs.
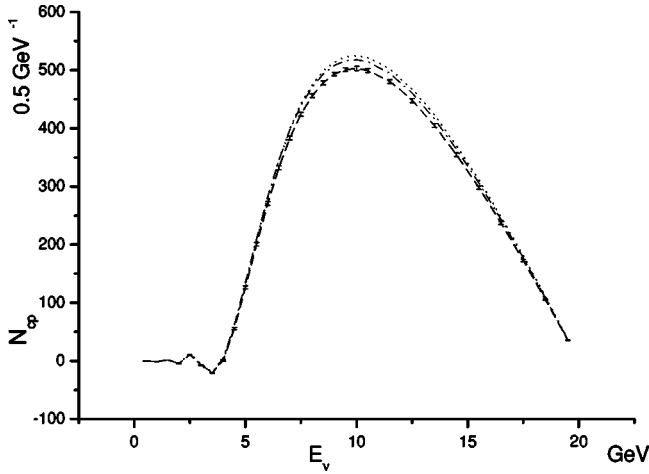
FIG. 5. Similar to Fig. 4 for the 2900 km baseline; the dashed curve is for $\delta_{cp}=0°$ and the error bars represent the weighted variation distribution with $r(x)=5\%$. The dotted line is the prediction of $\delta_{cp}=20°$ in the PREM, i.e., $r(x)=0$, while the dot-dashed line is given by $N_e(x)=(1+0.05)\hat{N}_e(x)$, where $\hat{N}_e(x)$ is given by the PREM.
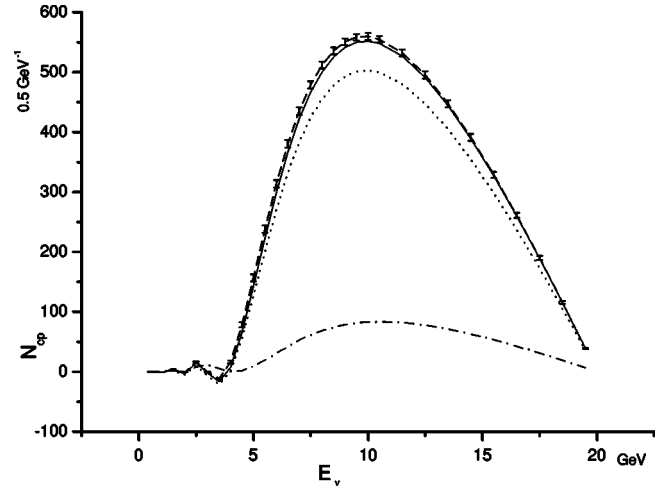

FIG. 6. The same plot as Fig. 4, but the *CP* parameter is chosen differently. The dashed line is for $\delta_{CP}=90°$ with error bars representing the uncertainties of $r=5\%$. The solid and dotted line are for $\delta_{CP}=54°$ and $0°$, respectively, with $r=0$, while the dash-dotted line is for $\delta_{CP}=90°$ in vacuum.

(21) and (13). The solid line without error bars is for a finite $\delta_{CP}=7.5°$. Clearly a small *CP* phase angle like 7.5° cannot be distinguished from a vanishing *CP* phase due to density uncertainty unless the *CP* phase angle is much larger.

We next consider the effect of constant density uncertainty of $r(x)=5\%$ given in Eqs. (11) and (19). In Fig. 5 the $\delta_{CP}=0$ line is again given by the dotted line together with the weighted variation distribution error bars given in Fig. 5. The dash-dotted curve is for $\delta_{CP}=0$ with the matter density $N_e(x)=(1+0.05)\hat{N}(x)$. This curve represents the 1σ upper bound in the fixed matter density uncertainty of 5% of the dashed curve. We see that the fixed matter density uncertainty gives a much larger error bar than that of the weighted variation distribution. It requires $\delta_{CP}>20°$, represented by the dotted curve, even at 1σ, in order to distinguish between the *CP* conserving and violating cases. Hence we see that according to the weighted variation distribution the uncertainty caused by that of the matter density is partially controllable, and the range of insensitivity of the measurement of *CP* effect at this baseline for small δ_{CP} is below 10° for a 1σ effect.

We show in Fig. 6 the cases of large *CP* violation. The dashed line is for $\delta_{CP}=90°$ for the PREM while the dot-dashed line is for $\delta_{CP}=90°$ in vacuum. The error bar on the $\delta_{CP}=90°$ curve is for the weighted variation distribution with $r=5\%$. The dotted line is in the PREM for $\delta_{CP}=0$ and the solid curve is for $\delta_{CP}=54°$ in the PREM. These results show that it is difficult to distinguish the large CPV of $\delta_{CP}=90°$ from $\delta_{CP}=54°$ in the presence of $r=5\%$ uncertainty in density. However, it can easily be distinguished from the *CP* conserving case (dotted line). The range of insensitivity, which is now about 36°, is larger than that for a smaller δ_{CP} discussed in the preceding paragraphs.

From Figs. 4, 5, and 6, we see that the matter effect in mimicking CPV is large. The range of insensitivity due to uncertainties in matter density depends on the value of δ_{CP}.

Figures 4 and 6 show that the best measurement at $L=2900$ km can be made at around $E=10$ GeV for the oscillating parameters given in Eq. (26). We note that the error bars depend mildly on the neutrino energy, and they are also bin size dependent as mentioned previously under Eq. (25) in the discussion of $\sigma_{\text{den},j}$.

We now investigate a much longer baseline. In Fig. 7 we plot N_{cp} vs the neutrino energy for a 12000 km baseline. We employ again the density uncertainty $r=5\%$. We also use a distance uncertainty scale of the average size, which is $\Delta x \simeq 100$ km, because the neutrino trajectory goes almost along Earth diameter. We take $E_\mu=50$ GeV to increase the statistics, but other conditions on the neutrino beam and the detector are unchanged. The solid curve is for $\delta_{CP}=90°$ and the dashed for $\delta_{CP}=0$. The error bars shown with the dashed curve of $\delta_{CP}=0$ are given for the weighted variation distribution of $r(x)=5\%$. The dash-dotted and dotted curves, calculated for $\delta_{CP}=90°$ with fixed Earth density uncertainties, Eqs. (11) and (19), are, respectively, for $N_e(x)=(1+0.05)\hat{N}_e(x)$ and $N_e(x)=(1-0.05)\hat{N}_e(x)$. One can see that the effect of the matter uncertainty is very large and it is difficult to distinguish $\delta_{CP}=90°$ from $\delta_{CP}=0°$ even in the weighted variation distribution at 1σ. The fixed matter uncertainty, represented by the broad region defining the dotted and dash-dotted curves, has no sensitivity to the *CP* phase. So in order to have sensitivity for the *CP* measurement at this very long baseline, the accuracy in the END has to be much better than 5%. We note that the error bars in Fig. 7 are larger than those at 2900 km. This shows a baseline dependence in $\sigma_{\text{den},j}$ as noted earlier. Hence extra care is needed in the treatment of the error if we measure CPV by combining the data from different lengths of baseline.

Figure 7 shows unequivocally that the fixed matter density uncertainty leads to a much larger error bar at very long baselines. The use of a fixed matter density uncertainty is
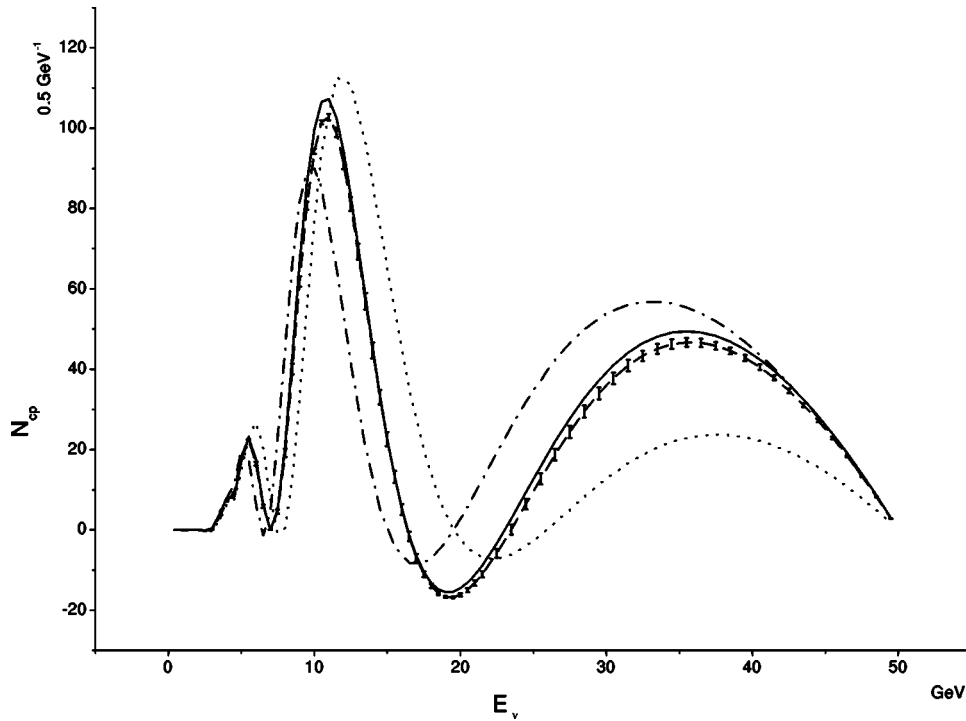
FIG. 7. The plot of CP-odd event number difference N_{CP} vs the neutrino energy E_ν for baseline $L=12000$ km. The dashed line is for $\delta_{CP}=0°$ with error bars representing $r=5\%$. The solid line is for $\delta_{CP}=90°$ with $r=0$. The dash-dotted and dotted lines are for $\delta_{CP}=90°$ and $N_e(x)=(1 \pm 0.05)\hat{N}_e(x)$, respectively, where $\hat{N}_e(x)$ is given by the PREM.

equivalent to our estimation with a very large uncertainty distance scale Δx that is the whole length of the baseline. This means that an unphysical correlation is imposed on the density uncertainties over different lattice sites along the neutrino trajectory. Hence we think it overestimates the effects of the uncertainty of the Earth density.

We have seen that the MSW effect can enhance the event numbers of the CP-odd difference and we also understand why the different sizes of the slices along the neutrino path as shown in Fig. 2 do not lead to some spurious MSW resonances. This is because they are too thin to produce a notable effect. The 2900 km baseline goes only as deep as the mantle and the density is still rather low even if a $r=5\%$ uncertainty is present. Near the earth center where density models are more precise, slices might rise higher or subside lower, but they are very narrow (merely about 100 km). These slices make $\tilde{D}_k$ in Eq. (20) differ from array to array, but most of them are close to each other. Rare large deviation happens according to Eq. (9), and they actually contribute less because of a large $K-1$ in Eq. (21).

IV. SUMMARY

To conclude, we have pointed out the uncertainty scale as a reference for the sensitive scale of interesting physics. Based on it we considered in some detail the issue of extract-

ing the information on the CPV effect in the presence of uncertainties in the Earth matter density in the light of high precision measurements anticipated in future LBL neutrino experiments. We have developed a formulation to estimate the error and analyzed how it affects the CP phase extraction. We have also presented a numerical implementation of the formulation and applied it to assess the effectiveness in the determination of the CP phase. We found that the CPV effect is more distinctly exhibited for the 2900 baseline than for the longest (12000 km). We have demonstrated that the use of fixed density uncertainty can lead to a much larger systematics error in the CP phase and this effect increases with the baseline due to the accumulative nature of the matter effect. In the case of the 12000 km baseline, the fixed density uncertainty renders the extraction of the CP phase almost impossible.

[1] G.L. Fogli and E. Lisi, Phys. Rev. D **54**, 3667 (1996); M. Tanimoto, *ibid.* **55**, 322 (1997); S.M. Bilenky, C. Giunti, and W. Grimus, *ibid.* **58**, 033001 (1998); V. Barger, S. Geer, and K. Whisnant, *ibid.* **61**, 053004 (2000); S. Parke and T.J. Weiler, Phys. Lett. B **501**, 106 (2001).

[2] L. Wolfenstein, Phys. Rev. D **17**, 2369 (1978); S.P. Mikheyev and A.Yu. Smirnov, Sov. J. Nucl. Phys. **42**, 913 (1985).

[3] J. Arafune, M. Koike, and J. Sato, Phys. Rev. D **56**, 3093 (1997); **60**, 119905(E) (1999); P. Lipari, *ibid.* **61**, 113004 (2000); C. Lunardini and A.Yu. Smirnov, *ibid.* **63**, 073009

(2001); J. Burguet-Castell, M.B. Gavela, J.J. Gomez-Cadenas, P. Hernandez, and O. Mena, Nucl. Phys. **B608**, 301 (2001).

[4] H. Minakata and H. Nunokawa, Phys. Rev. D **57**, 4403 (1998).

[5] M. Maris and S.T. Petcov, Phys. Rev. D **56**, 7444 (1997).

[6] M. Freund and T. Ohlsson, Mod. Phys. Lett. A **15**, 867 (2000), and references therein.

[7] J. Sato, Mod. Phys. Lett. A **14**, 1297 (1999); T. Ota and J. Sato, Phys. Rev. D **63**, 093004 (2001).

[8] A.M. Dziewonsky and D.L. Anderson, Phys. Earth Planet. Inter. **25**, 297 (1981).

[9] T. Ohlsson and H. Snellman, Eur. Phys. J. C **20**, 507 (2001).

[10] T. Ohlsson and W. Winter, Phys. Lett. B **512**, 357 (2001).

[11] R. Jeanlow and S. Morris, Annu. Rev. Earth Planet Sci. **14**, 377 (1986); R. Jeanlow, *ibid.* **18**, 357 (1990); Fu-Tian Liu *et al.*, Geophys. J. Int. **101**, 379 (1990); T.P. Yegorova *et al.*, *ibid.* **132**, 283 (1998); B. Romanowicz, Geophys. Res. Lett. **28**, 1107 (2001).

[12] G.E. Backus and J.F. Gilbert, Philos. Trans. R. Soc. London **A266**, 123 (1970); W. Menke, *Geophysical Data Analysis: Discrete Inverse Theory* (Academic, New York, 1984).

[13] D.D. Jackson, Geophys. J. R. Astron. Soc. **28**, 97 (1972); K. E. Bullen, *The Earth's Density* (Chapman and Hall, London, 1975).

[14] B.A. Bolt, Q. J. R. Astron. Soc. **32**, 367 (1991).

[15] Z. Maki, M. Nakagawa, and S. Sakata, Prog. Theor. Phys. **28**, 870 (1962); E.Kh. Akhmedov, S.T. Petcov, and A.Yu. Smirnov, Phys. Lett. B **309**, 95 (1993); Particle Data Group, D. Groom *et al.*, Eur. Phys. J. C **15**, 110 (2000).

[16] We follow the notation used in H.S. Chen *et al.*, ''Report of a Study on H2B, Prospect of a Very Long Baseline Neutrino Oscillation Experiment HIPA to Beijing,'' VLBL Study Group-H2B-1, Report No. IHEP-EP-2001-01, 2001, hep-ph/0104266, where the explicit form of *U* can be found.

[17] The quantum oscillation is a well-known time translation problem and expressing it as a time ordering operator is a standard approach. A discussion of this formulation can be found in Bing-Lin Young, ''Lecture Notes on Neutrino Oscillation,'' Beijing Summer School in Particle Physics, 2000.

[18] B.L.N. Kennet *et al.*, Geophys. J. R. Astron. Soc. **122**, 108 (1995); J.P. Montagner *et al.*, *ibid.* **125**, 229 (1995).

[19] F. Press, J. Geophys. Res. **73**, 5223 (1968).

[20] B.L.N. Kennett, Geophys. J. R. Astron. Soc. **132**, 374 (1998).

[21] A. Tarantola, *Inverse Problem Theory, Methods for Data Fitting and Model Parameter Estimation* (Elsevier, Amsterdam, 1987).

[22] The plot of the PREM as given in Fig. 2 was first given in M. Freund and T. Ohlsson, Mod. Phys. Lett. A **15**, 867 (2000).

[23] J. Pinney, talk given at the 3rd International Workshop on Neutrino Factory based on Muon Storage Rings (NuFACT01), Tsukuba, Japan, 2001, hep-ph/0106210.

[24] J. Burguet-Castell and O. Mena, hep-ph/0108109.

[25] V. Barger, K. Whisnant, and R.J.N. Phillips, Phys. Rev. Lett. **45**, 2084 (1980); M. Fukugita and M. Tanimoto, Phys. Lett. B **515**, 30 (2001).

[26] G.L. Fogli, E. Lisi, A. Marrone, and G. Scioscia, Phys. Rev. D **59**, 033001 (1999).

[27] Particle Data Group, [15], p. 198.

[28] B.A. Bolt and R.A. Uhrhmmer, Geophys. J. Int. **42**, 419 (1975).

[29] C. Albright *et al.*, ''Physics at a Neutrino Factory,'' hep-ex/0008064.

[30] V. Barger *et al.*, ''Oscillation Measurements with Upgraded Conventional Neutrino Beam,'' hep-ph/0103052.

[31] CHOOZ Collaboration, M. Apollonio *et al.*, Phys. Lett. B **420**, 397 (1998); **466**, 415 (1999); Super-K Collaboration, S. Fukuda *et al.*, Phys. Rev. Lett. **86**, 5651 (2001); SNO Collaboration, Q.R. Ahmad, *ibid.* **87**, 071301 (2001).